Journal of Non-Newtonian Fluid Mechanics, 40 (1991) 323–335
Elsevier Science Publishers B.V., Amsterdam

Corner flow of a suspension of rigid rods

R.A. Keiller and E.J. Hinch

Department of Applied Mathematics and Theoretical Physics, University of Cambridge, Cambridge CB3 9EW (UK)

(Received October 29, 1990; in revised form March 17, 1991)

Abstract

Stress singularities in the neighbourhood of sharp corners can be a source of severe problems in the numerical simulation of non-Newtonian flows leading to loss of convergence with grid refinement (G.G. Lipscombe, R. Kennings and M.M. Denn, J. Non-Newtonian Fluid Mech., 24 (1987) 85 [1]). For Newtonian flows the nature of this singularity is given by the analysis of Dean and Montagnon (W.R. Dean and P.E. Montagnon, Phil. Trans. R. Soc. London, Ser. A., 308 (1949) 199 [2]) in terms of similarity solutions. In this paper we extend this similarity analysis to a suspension of rigid rods. In the limit of nearly full extension the FENE constitutive model has the same behaviour as such a suspension. Our analysis predicts the possibility of lip vortices but their behaviour is somewhat inconsistent with those observed experimentally.

Keywords: corner flows; flow singularities; lip vortices; rigid rod suspensions

1. Introduction

The role of lip vortices in the flow of non-Newtonian fluids through abrupt contractions is a subject of much current interest. Experiments by Evans and Walters [3,4] suggest that lip vortices can be responsible for the vortex enhancement seen in these flows under certain experimental conditions.

These lip vortices are so-called because they occur at the lip of the $\frac{3}{2}\pi$ corner forming the contraction. Since the strain rate is singular at such a corner this presents difficulties in numerical simulations of contraction flows. For Newtonian fluids the flow in the neighbourhood of such a corner is well understood as the linearity of the Stokes' equation and its homogeneity in r, the radial coordinate, allow the streamfunction to be written as a summation over similarity solutions, as found by Dean and Montagnon [2]:

$$\psi = \sum_{i=1}^{\infty} r^{\lambda_i} f_i(\theta) \tag{1}$$

with $\lambda_1 = 1.545$, $\lambda_2 = 1.908, \ldots$

In general non-linearities in the constitutive equations used for the stress prohibit the use of such similarity solutions for non-Newtonian fluids. Henriksen and Hassager [5] have, however, obtained similarity solutions for the flow of a power-law fluid around a sharp corner. No lip vortices are observed in the neighbourhood of the corner in these solutions. These similarity solutions are possible because the stress is determined by the instantaneous strain rate. However, the power-law fluid model only describes shear thinning effects; there are no additional extensional or elastic stresses.

Davies [6] has examined the local behaviour of the corotational Maxwell model, which does incorporate elastic effects, near $r = 0$ in terms of a bi-orthogonal series expansion. In his analysis non-linearities in the stress equation lead to an infinite series of non-linear differential equations. Formally the solution of these equations may be written as a logarithmic series but the asymptotic behaviour near $r = 0$ is far from clear.

We consider in this paper the flow around a $\frac{3}{2}\pi$ corner of a suspension of non-Brownian rigid rods. For a given orientation of rods the stress is again linearly dependent on the instantaneous strain rate with a viscosity which is anisotropic and dependent on the rod orientation. The rod orientation is, itself, dependent on the flow field introducing convective non-linearities. However, if the rod orientation is independent of r and so only a function of the angular variable θ, similarity solutions are permissible reducing the non-linear partial differential equations to a non-linear ordinary differential eigenvalue problem. Some of our solutions do possess recirculating regions near the corner but there are some unsatisfactory features which will be discussed in Section 3.

2. Analysis and numerical calculation

We consider steady two-dimensional creeping flow near two plane boundaries meeting at an angle $\frac{3}{2}\pi$. Polar coordinates (r, θ) are taken centred on the corner with the plane boundaries at $\pm\frac{3}{4}\pi$. The velocity field is written in terms of a streamfunction, ψ, with the conditions of zero normal and tangential velocities on the plane boundaries $\theta = \pm \frac{3}{4}\pi$ being

$$\psi = \frac{\partial \psi}{\partial \theta} = 0. \tag{2}$$

The constitutive equation for a suspension of rigid rods in the limit of high aspect ratio and no Brownian motion is given by Batchelor [7,8] as

$$\sigma = -p\boldsymbol{I} + \mu(\nabla \boldsymbol{u} + \nabla \boldsymbol{u}^{\dagger}) + 2\mu\phi\boldsymbol{pp}(\boldsymbol{pp} : \nabla \boldsymbol{u}), \tag{3}$$

where $\boldsymbol{p}$, a unit vector, is the orientation of the rods given by

$$\frac{\mathrm{D}\boldsymbol{p}}{\mathrm{D}t} = \boldsymbol{p} \cdot \nabla \boldsymbol{u} - \boldsymbol{p}(\boldsymbol{p} \cdot \nabla \boldsymbol{u} \cdot \boldsymbol{p}) \tag{4}$$

and ϕ is the effective volume concentration of the rods given by

$$\phi = \frac{\pi n l^3}{12 \ln(l/a)}, \tag{5}$$

where n is the number density of rods, l their length and a their radius.

This constitutive equation is strictly valid only when the suspension is dilute in the sense that the rigid rods are non-interacting which requires $\phi \ll 1$. However, Batchelor [8] showed that the stress equation (eqn. (3)) has the same form for larger concentrations, at least in extensional flow, but with

$$\phi = \frac{\pi n l^3}{12 \ln(h/a)}, \tag{6}$$

where $h = (2nl)^{-1/2}$ is the average inter-rod spacing for a locally aligned distribution of rods.

Lipscomb et al. [9] used a similar set of equations using a formulation from Evans [10]. They were able to compute the flow of a suspension of glass fibres in an axisymmetric contraction in good agreement with experiments for values of ϕ up to 20. We will therefore assume that eqns. (3) and (4) hold for large values of ϕ.

In eqn. (3) the stress is linear in $\nabla \boldsymbol{u}$ but the viscosity depends on $\boldsymbol{p}$. As $\boldsymbol{p}$ is given by eqn. (4), the combined system of equations is non-linear in $\nabla \boldsymbol{u}$ and contains advection terms from eqn. (4). If the rod orientation $\boldsymbol{p}$ is independent of r, however, eqn. (3) becomes homogeneous in r, which then permits similarity solutions of the form $\psi = r^{\lambda} f(\theta)$ as for the Newtonian flow. The combined equations are still non-linear in $\boldsymbol{u}$, though, so summation over different similarity solutions is not permissible. In the momentum equation we ignore inertial and body forces so that the divergence of the stress (eqn. (3)) vanishes. Taking the curl of the momentum equation to eliminate the pressure, we obtain the following non-linear eigenvalue problem for λ

$$(1+\phi\delta^2)f''''$$
$$-\left\{\begin{array}{l} -\lambda^2(\lambda-2)^2-\left[\lambda^2+(\lambda-2)^2\right]f'' \\ +\phi\left\{\begin{array}{l}(2\lambda-\lambda^2)(\delta\Gamma+\epsilon\Delta-\zeta\delta)f \\ +\left[(\lambda-1)(\alpha\Gamma+\beta\Delta-\gamma\delta)+(2\lambda-\lambda^2)(\delta\Delta-2\epsilon\delta)\right]f' \\ +\left[-(2\lambda-\lambda^2)\delta^2+(\lambda-1)(\alpha\Delta-2\beta\delta)+\delta\Gamma+\epsilon\Delta-\zeta\delta\right]f'' \\ +\delta\left[\Delta-2\epsilon+(1-\lambda)\alpha\right]f'''\end{array}\right\}\end{array}\right\}$$
$$=0, \tag{7}$$

where $\boldsymbol{p}=[p_r(\theta),\ p_\theta(\theta)]$ and

$$\alpha=p_r^2-p_\theta^2,\ \beta=\alpha',\ \gamma=\alpha'',\ \delta=p_rp_\theta,\ \epsilon=\delta',\ \zeta=\delta'',$$
$$\Gamma=\lambda(\lambda-2)\delta-(\lambda-1)\beta-\zeta,\ \Delta=-(\lambda-1)\alpha-2\epsilon.$$

2.1. *Aligned orientation*

Equation (4) for the orientation of the rods may be re-expressed as

$$\boldsymbol{p}=\frac{\boldsymbol{q}}{|\boldsymbol{q}|}, \tag{8}$$

with $\boldsymbol{q}$ satisfying

$$\frac{\mathrm{D}\boldsymbol{q}}{\mathrm{D}t}=\boldsymbol{q}\cdot\nabla\boldsymbol{u}. \tag{9}$$

Equation (9) is the equation for the evolution of a line element and therefore has $\boldsymbol{q}=\boldsymbol{u}$ as one solution. As the rods are aligned with the streamlines in this solution, we will refer to this as the aligned orientation for the rods. Now if $\boldsymbol{u}$ is given by a similarity solution then $\boldsymbol{p}$ is indeed independent of r as required for such a similarity solution.

It is important to note the necessary conditions for the stability of this rod orientation. The criterion for the stability of this orientation is given by Lipscomb et al. [9] as

$$\boldsymbol{u}\cdot\nabla\boldsymbol{u}\cdot\boldsymbol{u}-\boldsymbol{v}\cdot\nabla\boldsymbol{u}\cdot\boldsymbol{v}>0, \tag{10}$$

where $\boldsymbol{u}\cdot\boldsymbol{v}=0$ and $\boldsymbol{u}$ and $\boldsymbol{v}$ are of equal magnitude. In planar flow this requires that the fluid is accelerating in the direction of the velocity which is satisfied in the bulk flow in a contraction. In shear flows there is no acceleration of the flow but the rods still align with the streamlines.

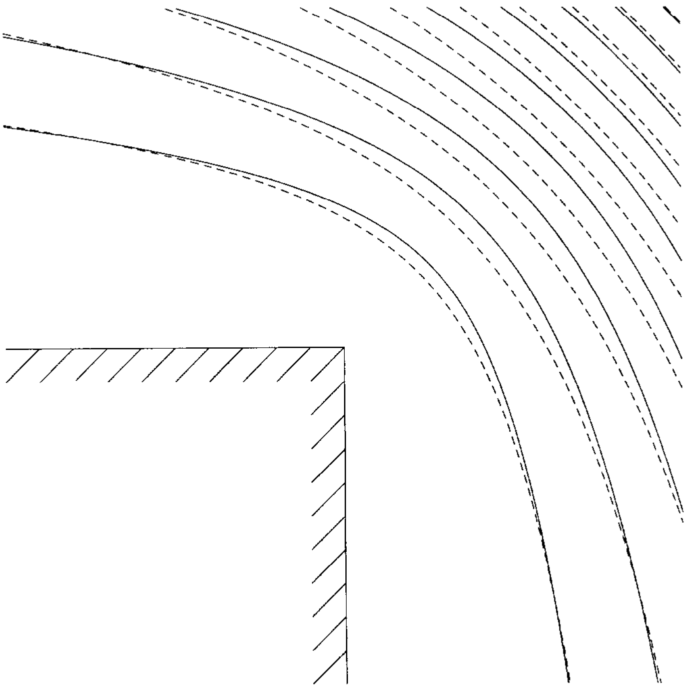

Fig. 1. Antisymmetric aligned flows around $\frac{3}{2}\pi$ corner for $\phi = 0$ (Newtonian flow) - - - - - - and for $\phi = 10$ ———.

In the lowest mode of the Newtonian flow, fluid particles approach the corner from $\theta = -\frac{3}{4}\pi$ in a shear flow and accelerate until they reach $\theta = 0$ (Fig. 1). We therefore assume that in such a flow the rods would be aligned along the streamlines by the shearing flow near $\theta = -\frac{3}{4}\pi$ and by the extensional flow in the bulk of the contraction. They will remain aligned with the streamlines until they approach $\theta = \frac{3}{4}\pi$. Consequently we examine the solution of eqn. (7) assuming this aligned orientation, increasing ϕ and starting from the lowest mode of the Newtonian flow. For the orientation of the rods we now have

$$(p_r, p_\theta) = \frac{(\psi_\theta, -\psi_r)}{|(\psi_\theta, -\psi_r)|} = \frac{(f', -\lambda f)}{|(f', -\lambda f)|}, \tag{11}$$

and substitution into eqn. (7) yields, after rearrangement,

$$f'''' = \frac{\left\{ \begin{array}{l} -\left[(\lambda-2)^2+\lambda^2\right] f'' - \lambda^2(\lambda-2)^2 f \\ +\phi \left[\begin{array}{l} \lambda^3 gff' + \lambda^2(\lambda-1)g'f^2 + (\lambda+2)gf'f'' \\ +\lambda gff''' + (\lambda+1)g'f'^2 + 2\lambda g'ff'' + \lambda hf'f \end{array} \right] \end{array} \right\}}{\left[1+\phi\lambda^2 f^2 f'^2/\left(f'^2+\lambda^2 f^2\right)^2\right]}, \tag{12}$$

where

$$g = \frac{\left[(\lambda - 1)f'^3 - \lambda f f' f'' - \lambda f^2 f'\right]}{\left[f'^2 + \lambda^2 f^2\right]^2} \tag{13}$$

and

$$h = g'' - \frac{\lambda f f' f''''}{\left[f'^2 + \lambda^2 f^2\right]^2}. \tag{14}$$

As f and f' both vanish at $\theta = \pm \frac{3}{4}\pi$ the denominator of eqn. (12) vanishes. A Taylor series expansion is therefore used at $\theta = \pm \frac{3}{4}\pi$ to give

$$f''''(\pm \tfrac{3}{4}\pi) = \left[-(\lambda - 2)^2 - \lambda^2 + \phi\left(\frac{\lambda}{2} - 1\right)\right] f''(\pm \tfrac{3}{4}\pi). \tag{15}$$

These equations have been solved by numerical integration using a fourth-order Runge–Kutta scheme with a variable step-size and a shooting technique for the eigenvalue λ. The shooting parameters, λ and f'', were varied at $\theta = \frac{3}{4}\pi$ (f''' may be normalized to unity at $\theta = \frac{3}{4}\pi$) until both f' and f''' vanished at $\theta = 0$. In this way flows antisymmetric about $\theta = 0$ were found for values of ϕ from 0 to 180 (symmetric streamfunctions produce antisymmetric flows). Attempts to find asymmetric flows were unsuccessful.

For $\phi < 137$ these solutions are similar to the lowest mode of the Newtonian flow. For example, the flow for $\phi = 10$ is shown together with the Newtonian flow in Fig. 1. The value of λ for these solutions is slightly greater than for the Newtonian flow, rising from the Newtonian value of 1.545 at $\phi = 0$ to 1.683 at $\phi = 130$ indicating that these flows are slightly less singular. Figure 2 shows this variation of λ with ϕ.

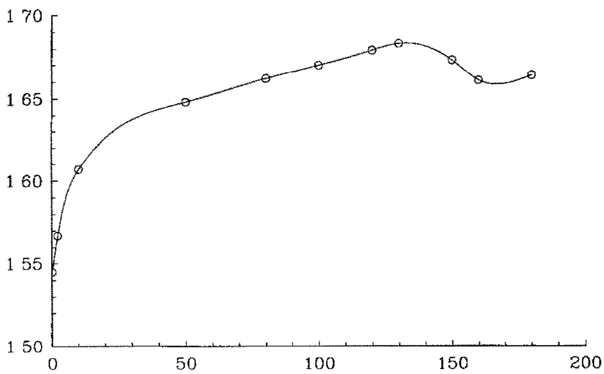

Fig. 2. Eigenvalue λ as a function of ϕ for the aligned solutions.

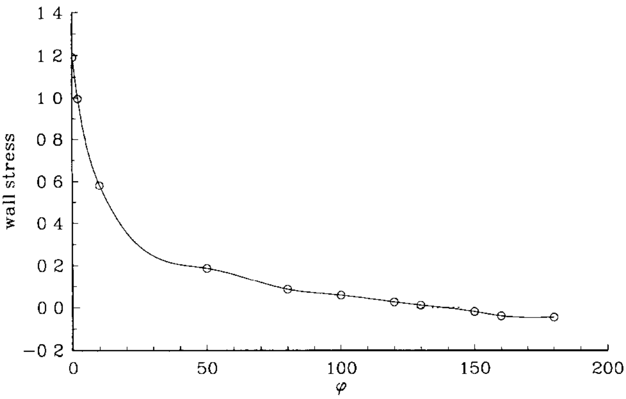

Fig. 3. The wall shear rate, $f''(\frac{3}{4}\pi)$, for the aligned solutions as a function of ϕ.

At $\phi \approx 137$, the wall shear rate, $f''(\frac{3}{4}\pi)$, changes sign as seen in Fig. 3 For $\phi > 137$ the flow now possesses two recirculating regions, symmetrically either side of the corner, as in the flow for $\phi = 180$ shown in Fig. 4. λ remains around 1.67 for these flows.

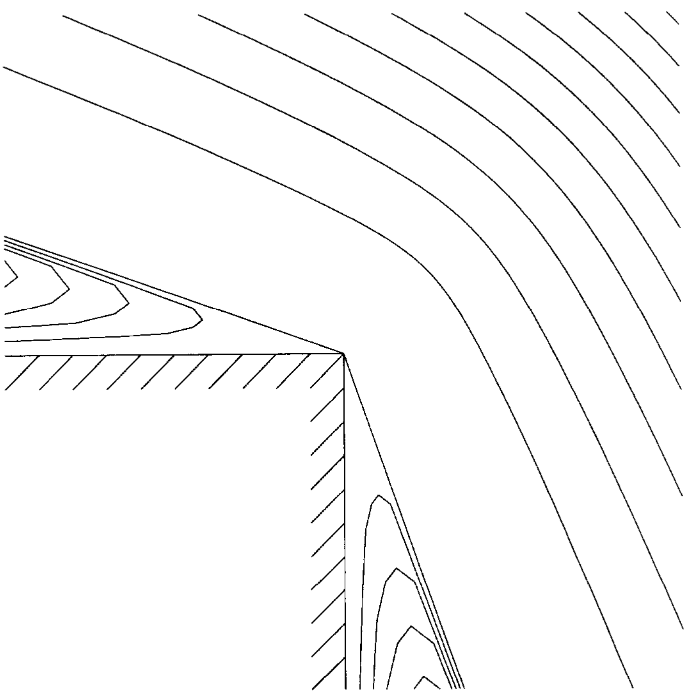

Fig. 4. Streamlines for the aligned flow at $\phi = 180$. The increments between the bulk streamlines are 1000 times the increments between the recirculating streamlines.

Thus flows have been obtained with recirculating regions. However, the recirculations are present on both the upstream and downstream sides of the corner. Further the alignment assumption of the rods is now no longer appropriate in the corner region. Fluid approaching the corner along the separating streamline is decelerating and so the rods will not align with the streamlines.

2.2. De-aligned orientation

We now reconsider eqn. (9) for flows past a corner where recirculation is present on the upstream side of the corner. Assuming that such a flow may still be described by a similarity form, f vanishes on the separating streamline and along this streamline eqn. (9) becomes

$$f'\frac{\partial q_r}{\partial r} = (\lambda - 1)f'q_r + f''q_\theta, \tag{16}$$

$$f'\frac{\partial q_\theta}{\partial r} = (1 - \lambda)f'q_\theta. \tag{17}$$

The two solutions of these equations for the orientation of the rods are $(q_r, q_\theta) = r^{\lambda-1}(1, 0)$ and $r^{1-\lambda}[f'', 2(1-\lambda)f']$. The first solution is again the aligned solution which, for $\lambda > 1$, decays as $r \to 0$ showing that it is unstable. The second solution grows as $r \to 0$ and is therefore the orientation which an initially random distribution of rods will adopt as they are advected towards $r = 0$. Thus, in the neighbourhood of $r = 0$, and along the separating streamline, we have

$$\boldsymbol{p} = \frac{\boldsymbol{q}}{|\boldsymbol{q}|} = \frac{[f'', 2(1-\lambda)f']}{|[f'', 2(1-\lambda)f']|}. \tag{18}$$

The orientation of the rods in the rest of the flow domain may now be found by the substitution of $\boldsymbol{q} = r^{(1-\lambda)}[Q_r(\theta), Q_\theta(\theta)]$ into eqn. (9) with $Q_r = f''$ and $Q_\theta = 2(1-\lambda)f'$ on the separating streamline. This gives

$$\lambda f Q_r' = -2(\lambda - 1)f'Q_r - f''Q_\theta, \tag{19}$$

$$Q_\theta' = (\lambda - 2)Q_r. \tag{20}$$

We call the resulting orientation, $\boldsymbol{p}$, the de-aligned orientation. This orientation is also independent of r so similarity solutions for ψ are indeed still permitted.

This orientation is appropriate to symmetric flows such as the second mode of the Newtonian flow. We therefore solved eqns. (7) (18) (19) and (20) for $f(\theta)$ antisymmetric about $\theta = 0$. Again these equations were solved as a shooting problem by integrating numerically from $\theta = 0$ to $\theta = \frac{3}{4}\pi$ with

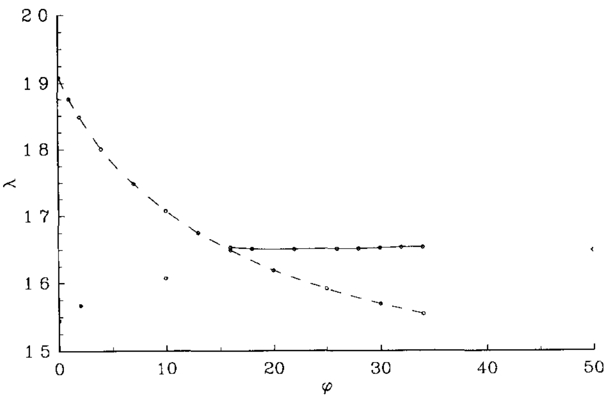

Fig. 5. Eigenvalue λ as a function of ϕ for the aligned solutions - - - - - -, the symmetric de-aligned solutions — — — and the asymmetric de-aligned solutions ———.

initial conditions $f(0)=0$, $f'(0)=1$, $f''(0)=0$ and with $f'''(0)$ and λ varied until f and f' both vanished at $\theta=\frac{3}{4}\pi$.

In contrast to the antisymmetric flows λ decreases with ϕ for these solutions indicating that the flow is more singular at $r=0$ than the corresponding Newtonian flow. Beyond $\phi \approx 18$ these flows become more singular than the antisymmetric flows for the same ϕ. The values of λ for these flows are shown in Fig. 5.

We have also been able to obtain asymmetric flows with this de-aligned rod orientation. Finding such flows is a shooting problem in three parameters as f'' no longer vanishes on the separating streamline. As the position of the separating streamline is also not known in advance for a general asymmetric flow this must also be determined as part of the solution. The following procedure was therefore adopted.

Changing the origin of the θ variable, let the separating streamline be at $\theta=0$. Now, integrating the equations away from $\theta=0$, let $-\alpha[\lambda, f''(0), f'''(0)]$ be the first value of θ at which $f(\theta)=0$ for $\theta<0$. λ, $f''(0)$ and $f'''(0)$ are now varied until $f'(-\alpha)=f(\frac{3}{2}\pi-\alpha)=f'(\frac{3}{2}\pi-\alpha)=0$. Returning to the original origin for θ the separating streamline is at $\theta=-\frac{3}{4}\pi+\alpha$.

In this way asymmetric flows were found for $\phi=16$–34. Figure 6 shows the variation of the recirculation angle, the angle between the separating streamline and $\theta=-\frac{3}{4}\pi$, with ϕ. As ϕ is reduced towards 16 this angle increases rapidly reaching $\frac{3}{4}\pi$ at a value of ϕ just less than 16. Thus these solutions arise as a result of a bifurcation of the antisymmetric flow at $\phi \approx 16$. Solutions have not been pursued beyond $\phi=34$ but there is a possibility that at $\phi \approx 137$ the recirculation will vanish and the same flow as the aligned flow will be obtained since the initial conditions $f(-\frac{3}{2}\pi)=f'(-\frac{3}{2}\pi)=f''(-\frac{3}{2}\pi)=0$, $f'''(\frac{3}{2}\pi)\neq 0$ are appropriate for an asymmetric

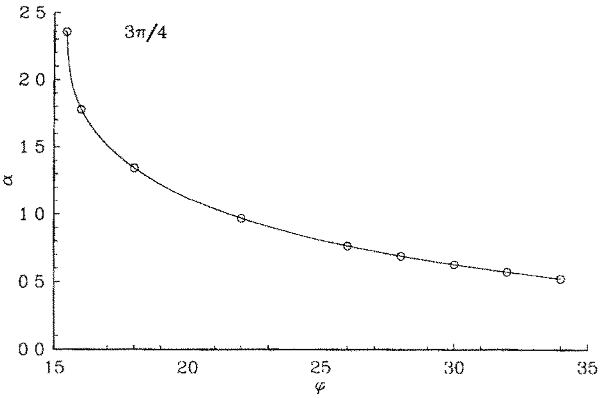

Fig. 6. Recirculation angle for the asymmetric de-aligned solutions as a function of ϕ.

recirculating flow in the limit where the recirculation vanishes. The flows for $\phi = 18$ and 32 are shown in Figs. 7 and 8. For these solutions λ remains approximately 1.65, close to the antisymmetric aligned flows but greater than the symmetric flows with the de-aligned orientation. Again these values of λ are included in Fig. 5.

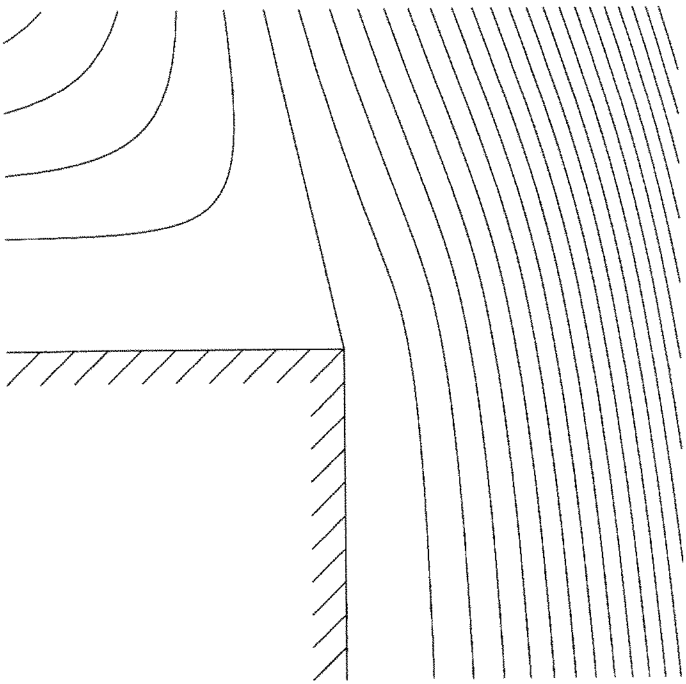

Fig. 7. Streamlines for the asymmetric de-aligned flow at $\phi = 18$.

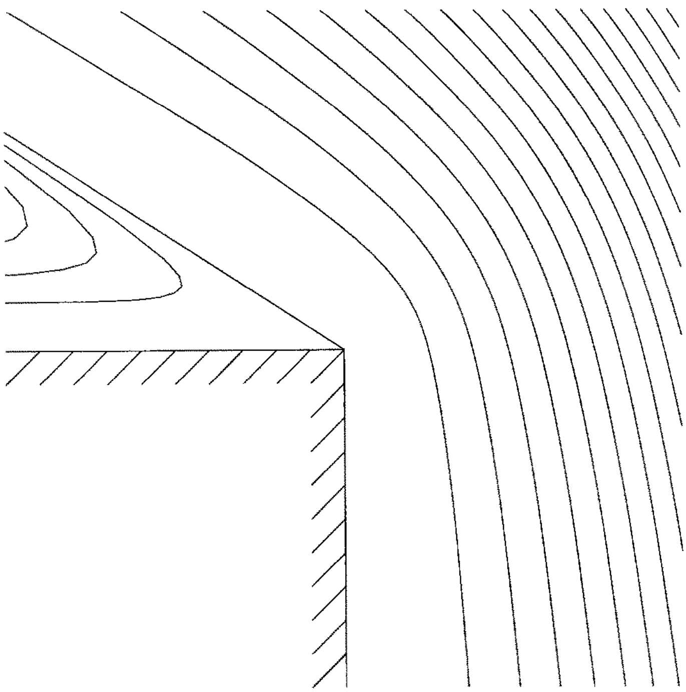

Fig. 8. Streamlines for the asymmetric de-aligned flow at $\phi = 32$. Increments between the bulk streamlines are 20 times the increments between the recirculating streamlines.

Alternative alignment assumptions have also been considered, for example with the aligned orientation for rods moving past the corner and the de-aligned orientation in the recirculating region. These solutions are qualitatively similar to the de-aligned solutions.

3. Discussion

Qualitatively at least we would expect a dilute polymer solution to behave similarly to a suspension of rigid rods in the neighbourhood of a flow singularity such as a $\frac{3}{2}\pi$ corner. If the flow is strong enough to fully unravel the polymers then their contribution to the stress (as described for example by a FENE dumbbell) will be viscous in nature just as in a suspension of rigid rods. This would occur at least while the flow is still trying to stretch the polymers; fully extended polymer chains would not exert any stresses to resist compression as rigid rods would.

We have found solutions for the flow of a suspension of rigid rods around a sharp $\frac{3}{2}\pi$ corner corresponding to the lowest two modes of the Stokes' flow. These solutions require the orientation of the rods to be independent of r and in either the aligned or the de-aligned orientation. At least for $\phi < 34$ these solutions are consistent with the alignment assumptions adopted. At $\phi \approx 16$ the symmetric flows bifurcate to produce an additional asymmetric flow. This flow possesses a recirculating region on one side of the corner which could be considered as part of a lip vortex similar to the vortices observed by Evans and Walters [3,4] and others. However there are certain unsatisfactory features of these solutions.

We have found that the recirculation angle of the asymmetric flows decreases with increasing ϕ. This is in contrast to the series of experiments reported by Lipscomb et al. [9] for a suspension of glass fibres in a 4:1 contraction. The angle of recirculation at the corner in these experiments increases with the concentration of glass fibres for $0 < \phi < 20$. However our analysis is valid only in a very small neighbourhood of the corner, as the rods must experience the flow for long enough to adopt the de-aligned orientation. In such a small region the finite length of the glass fibres used by Lipscomb et al. makes eqns. (3) and (4) inappropriate. We suggest therefore that the vortices observed by Lipscomb et al. are a consequence of the contraction flow and not the flow singularity.

As the underlying problem is non-linear it is not permissible to write the general solution of eqns. (3) and (4) as a summation over different solutions. Furthermore the eigenvalues, λ, for all three possible solutions are very similar, indeed the symmetric flow becomes slightly more singular than the antisymmetric flow for $\phi > 18$. Therefore it is not clear from this local analysis what the flow will look like near $r = 0$ and further information about the main flow may be required to determine whether lip vortices will be seen. From the point of view of numerical simulations of the full contraction flow, we can at least expect the singularity at $r = 0$ to be comparable if not slightly weaker than in a Newtonian flow.

Acknowledgement

R.A.K. is grateful to the British Petroleum Company PLC for financial support.

References

1 G.G. Lipscomb, R. Keunings and M.M. Denn, J. Non-Newtonian Fluid Mech., 24 (1987) 85–96.
2 W.R. Dean and P.E. Montagnon, Phil. Trans. R. Soc. London Ser. A., 308 (1949) 199–218.
3 R.E. Evans and K. Walters, J. Non-Newtonian Fluid Mech., 20 (1986) 11–29.
4 R.E. Evans and K. Walters, J. Non-Newtonian Fluid Mech., 32 (1989) 95–105.
5 P. Henriksen and O. Hassager, J. Rheol., 33 (1989) 865–879.

6 A.R. Davies, J. Non-Newtonian Fluid Mech., 29 (1988) 269–294.
7 G.K. Batchelor, J. Fluid Mech., 41 (1970) 545–570.
8 G.K. Batchelor, J. Fluid Mech., 46 (1971) 813–829.
9 G.G. Lipscomb, M.M. Denn, D.U. Hur and D.V. Boger, J. Non-Newtonian Fluid Mech., 26 (1988) 297–325.
10 J.G. Evans, Ph.D. Thesis, Cambridge University, 1975.